Mar Geophys Res (2007) 28:59–79
DOI 10.1007/s11001-007-9014-9

ORIGINAL RESEARCH

Structures of the northeasternmost South China Sea continental margin and ocean basin: geophysical constraints and tectonic implications

Chun-Feng Li · Zuyi Zhou · Jiabiao Li · Hujun Hao · Jianhua Geng

Received: 19 June 2006 / Accepted: 25 January 2007 / Published online: 6 March 2007
© Springer Science+Business Media B.V. 2007

Abstract The northeastern part of the South China Sea is a special region in many aspects of its tectonics. Both recent drilling into the Mesozoic and new reflection seismic surveys in the area provide a huge amount of data, fostering new understanding of the continental margin basins and regional tectonic evolution. At least four half-grabens are developed within the Northern Depression of the Tainan Basin, and all are bounded on their southern edges by northwestward-dipping faults. One of the largest half-grabens is located immediately to the north of the Central Uplift and shows episodic uplift from the late Oligocene to late Miocene. Also during that period, the Central Uplift served in part as a material source to the Southern Depression of the Tainan Basin. The Southern Depression of the Tainan Basin is a trough structure with deep basement (up to 9 km below sealevel or 6 km beneath the sea bottom) and thick Cenozoic sedimentation (>6 km thick). Beneath the Southern Depression we identified a strong landward dipping reflector within the crustal layer that represents a significant crustal fault. This reflector coincides with a sharp boundary in crustal thicknesses and Moho depths. We show that the northeasternmost South China Sea basin, which may have undergone unique evolution since the late Mesozoic, is markedly different from the central South China Sea basin and the Huatung Basin, both geologically and geophysically. The Cenozoic evolution of the region was largely influenced by pre-existing weaknesses due to tectonic inheritance and transition. The South China Sea experienced multiple stages of Cenozoic extension.

Keywords Crustal structure · Deep crustal reflector · Episodic rifting · Gravity modeling · Seismic stratigraphy · South China Sea · Tainan basin

C.-F. Li (✉) · Z. Zhou · J. Geng
School of Ocean and Earth Sciences, Tongji University, Shanghai 200092, China
e-mail: cfl@mail.tongji.edu.cn

J. Li
2nd Institute of Oceanography, State Oceanic Administration, Hangzhou 310012, Zhejiang, China

H. Hao
Nanhai East Institute of CNOOC Research Center, Guangzhou 510240, Guangdong, China

Introduction

The tectonic evolution of the northeastern part of the South China Sea (Figs. 1 and 2) has been both intriguing and perplexing. Its magnetic anomaly patterns are very quiet compared to the central South China Sea basin (Fig. 3). It is therefore somewhat difficult to interpret the northeasternmost South China Sea as having the same origin as the central South China Sea basin, which is widely accepted to be formed by Paleogene continental rifting (~58–30 Ma) and subsequent oceanic floor spreading during the Oligo-Miocene (~30–15 Ma) (Holloway 1982; Su et al. 1989; Clift and Lin 2001; Lin et al. 2003). Sibuet and Hsu (1997), and Sibuet et al. (2002, 2004) argued that prior to 15 Ma the Ryukyu subduction zone extended south to the northeasternmost South China Sea, and that the Northern Depression of the Tainan Basin is a remnant of that subduction system. These authors consequently interpreted a sector of the northeasternmost South China Sea as oceanic crust that differs from the central South China Sea crust,

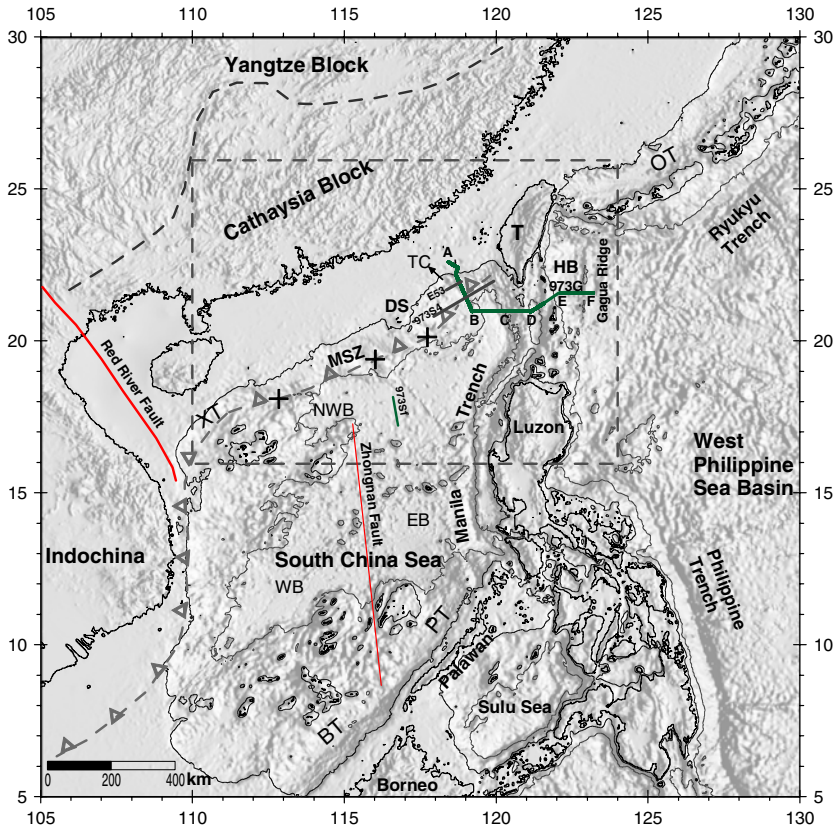

Fig. 1 Shaded relief map showing major tectonic regimes in the South China Sea region. Line ABCDEF is the transection surveyed by GMGS. The dashed square outlines the area shown in Fig. 2. Two isobaths shown on the map are 500 m and 3,000 m, respectively. BT = Borneo Trough; DS = Dongsha Rise; HB = Huatung Basin; MSZ = suggested Mesozoic subduction zone; EB = east sub-basin; WB = west sub-basin; NWB = northwest sub-basin; OT = Okinawa Trough; PT = Palawan Trough; T = Taiwan; TC = Taiwan Canyon; XT = Xisha Trough. + symbols indicate the sites of highly reflective throughgoing crustal faults from Hayes et al. (1995)

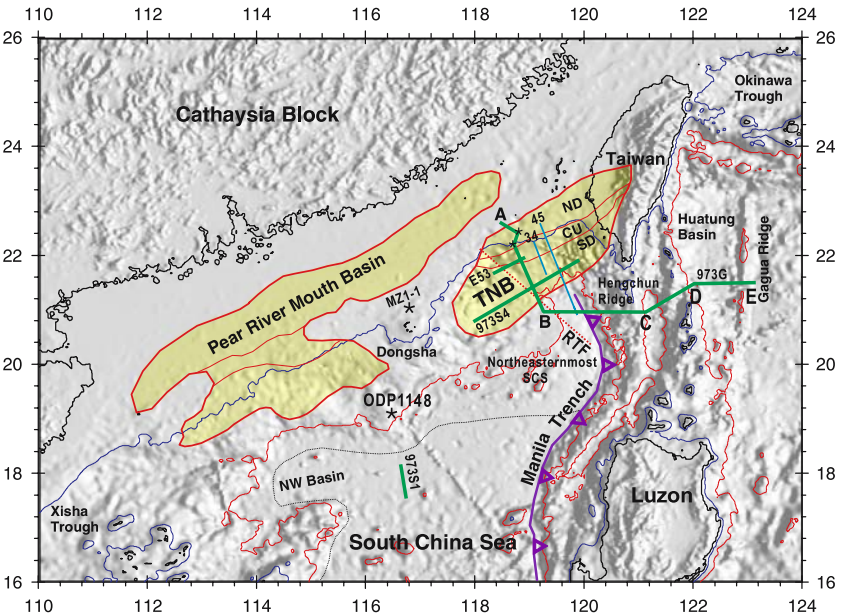

Fig. 2 Shaded relief map outlining the Tainan Basin and Pearl River Mouth Basin. Two isobaths shown on the map are 500 m and 3000 m, respectively. TNB = Tainan Basin; ND = Northern Depression; CU = Central Uplift; SD = Southern Depression; RTF = relict transform fault; * = well drilling site; NW Basin = northwestern South China Sea sub-basin; 973G, 973S1, 973S4, E53, 34, and 45 are seismic lines. Dashed line shows the continent-ocean boundary of the South China Sea estimated from regional magnetic (Fig. 3) and reflection seismic data

but which may have some genetic relationships to a portion of the present-day Huatung Basin. In contrast, the northern South China Sea passive margin may have extended further to the northeast of Taiwan about 10 Ma (Teng 1990, 1996; Clift et al. 2003; Hall 2002).

The regional magnetic anomaly map (Fig. 3) shows several interesting features. The Cathaysian block has relatively high magnetic anomalies, which are commonly interpreted as being caused by volcanisms linked to paleo-Pacific plate subduction (Zhou and Li 2000). Within the central South China Sea basin, magnetic belts from oceanic floor spreading show clear differences between the western and the eastern sub-basins (Fig. 1). Within the western sub-basin the

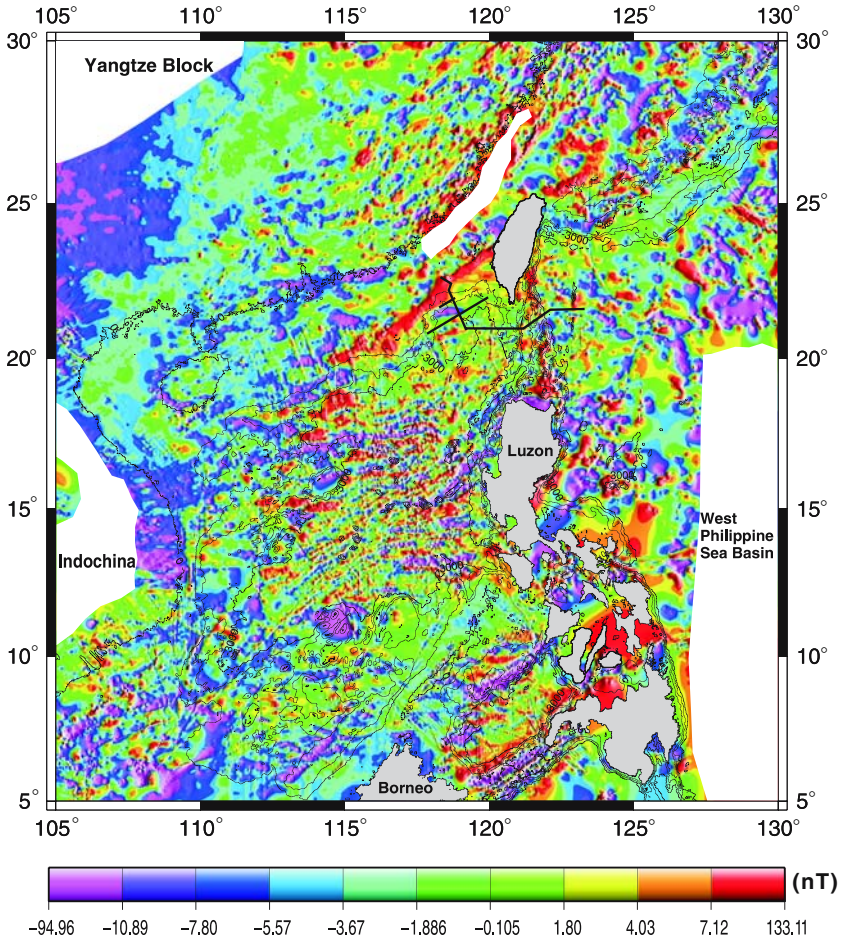

Fig. 3 Magnetic anomaly map of the South China Sea and surrounding regions, overlapped with isobath contours. Magnetic data from Geological Survey of Japan (1996)

magnetic anomaly belts are narrower and have lower amplitudes, but anomaly belts in the eastern sub-basin are wider and have stronger undulations. This magnetic difference may either support an episodic rifting of the South China Sea (Ru and Pigott 1986), or can be attributed to different crustal types where the western and eastern sub-basins evolved independently. Pautot et al. (1986) suggested that the eastern sub-basin developed as earlier oceanic crust, whereas the western sub-basin resulted from continental rifting and subsequent oceanic floor spreading. As such, the ancient oceanic crust formed before the sea floor spreading of the eastern South China Sea sub-basin deserves further study. From the distribution of the magnetic belts within the eastern sub-basin and their geometrical relationships to the continental margin, it has been argued that opening of the eastern sub-basin was at least partially within older oceanic crust, probably the paleo-Pacific plate, and that the northeasternmost South China Sea is the most likely place to preserve the paleo-Pacific crust (Xia et al. 1997).

Although the aforementioned two camps of scientists based their arguments on two different subduction systems, i.e., a Cenozoic Ryukyu subduction and a Mesozoic paleo-Pacific subduction, respectively, most share the common ground that the northeasternmost South China Sea is different from the central South China Sea. However, based on magnetic anomaly interpretations, Briais et al. (1993) argued that the South China Sea ocean basin was formed in a single episode of rifting, a model which is later supported by Teng (1996) and Clift et al. (2003). Extensive studies on the deep structures and rifting have been made offshore the Pearl River Mouth Basin (Nissen et al. 1995a; Clift and Lin 2001; Clift et al. 2002). To the northeast, additional information is needed to further pinpoint the nature of the crust in the northeasternmost South China Sea, which is key to regional geodynamic reconstructions.

In addition, the Chinese continental margin is characterized by pairs of NE-trending basement depressions and uplifts covered with Cenozoic

sedimentary layers. These depressions and uplifts are attributed to either continental margin rifting or oceanic floor subduction, but their exact formation mechanisms still remain ambiguous. Because basin-uplift pairs dominate the basement structure of the region, detailed studies on them are therefore vital for understanding early continental margin evolution. In this regard we need better mapping of the basement configuration beneath the Cenozoic sedimentary rocks and to examine the deeper crustal structures of this area. The discovery of oil and gas from Lower Cretaceous shallow marine facies in the Northern Depression of Tainan Basin sets additional commercial importance on such studies, as increasing attentions are being paid to Mesozoic hydrocarbon potentials offshore China.

In 2001, two geophysical expeditions were made to survey the South China Sea and surrounding regions. The first survey was carried out by Guangzhou Marine Geological Survey (GMGS) of the Chinese Ministry of Land and Resources. From the west to the east, this traversed the Chinese continental shelf/slope, the northeastern part of the South China Sea, the Manila Trench and Manila accretionary prism, the Luzon Arc, the Huatung Basin and the Gagua Ridge (Fig. 1). In the second survey, made by the South China Sea Institute of Oceanology (SCSIO) of the Chinese Academy of Sciences, multiple seismic lines were shot on the northern South China Sea continental margin and within the South China Sea deep sea basin (Fig. 1). Collectively about 2,850 km of multichannel seismic lines, with integrated gravimetric, magnetic and bathymetric measurements were collected.

For evaluating hydrocarbon potential in Mesozoic rocks, Chinese National Offshore Oil Company (CNOOC) in 2003 drilled the first deep well (MZ1-1) ever targeted for the Mesozoic on the northern South China Sea continental margin (Fig. 2). Drilling and logging data revealed new information on Upper Mesozoic rock types, their geophysical properties and paleo-environments. Using these new data, we focus on the study of basement morphologies, tectonic styles, and crustal density structures of the northeasternmost South China Sea and surrounding regions. Regional post-Cretaceous tectonic evolution is further inferred from these new geophysical constraints.

Regional tectonic scheme

The Chinese continental margin around Taiwan (Fig. 1) is at the junction of four major tectonic regimes of distinct evolutionary histories. To its immediate west lies the Cathaysian fold belt, commonly known as a Mesozoic magmatic arc system due to the subduction of the paleo-Pacific plate beneath the Eurasia plate from the mid-Jurassic to Cretaceous (Jahn et al. 1976; Hamilton 1979; Gilder et al. 1996; Zhou et al. 1996; Lapierre et al. 1997; Chen and Jahn 1998; Zhou and Li 2000). Starting from about 50 Ma, the southern Chinese continental margin changed its tectonic regime from subduction to continental stretching and rifting, which eventually led to the opening of the South China Sea during the late Oligocene (Taylor and Hayes 1980, 1983; Holloway 1982; Su et al. 1989; Clift and Lin 2001).

To the northeast of Taiwan extends the NE-trending Ryukyu Trench-Ryukyu volcanic arc-Okinawa Trough system (Fig. 1), where the Philippine Sea plate is subducting in a NW direction along the Ryukyu Trench, and the Okinawa Trough is undergoing active back-arc rifting (Kizaki 1986; Miki 1995; Sibuet and Hsu 1997; Shinjo 1999; Wang et al. 1999). Although this active subduction and back-arc rifting process has started only recently since the late Cenozoic (Kizaki 1986; Lee and Lawver 1995) owing to the northward and clockwise movement of the Philippine Sea plate (Hall et al. 1995; Hall 2002), it is generally argued from the distribution of Cathaysian magmatism that the Mesozoic paleo-Pacific subduction might have also followed roughly along the present-day Ryukyu Trench and northern South China Sea continental margin.

The Philippine Sea plate, bounded by active subduction zones, has itself a long and complicated multi-phase history (Hall et al. 1995; Hall 2002). The Huatung Basin located east of Taiwan was proposed as a trapped fragment of the Cretaceous 'proto-South China Sea' or the 'New Guinea Basin' within the Philippine Sea plate (Deschamps et al. 2000). The Gagua Ridge between the Huatung Basin and the Philippine Sea plate acted as a transverse plate boundary accommodating the northwest shear motion of the Philippine Sea plate (Sibuet and Hsu 1997; Deschamps et al. 1998, 2000; Sibuet et al. 2002).

The Luzon Arc to the east and southeast Taiwan formed behind the Manila Trench as the South China Sea plate started subducting beneath the Philippine Sea plate about 15 Ma (Briais et al. 1993; Yang et al. 1996). As the Luzon Arc migrated progressively to the west (Seno et al. 1993), it started to collide either with the Eurasian continental margin (Suppe 1984; Ho 1986; Teng 1990; Chemenda et al. 2001; Clift et al. 2003) or with the pre-existing Ryukyu Arc (Hsu and Sibuet 1995). And it is generally argued that the Taiwan orogen, one of the youngest in the world, is the outcome of this collision process. The Luzon Arc first

began to strike mid-Taiwan along the Longitudinal Valley in an oblique angle, and the collision then progressively propagated to the south (Davis et al. 1983; Suppe 1984), causing present-day active collision in southern Taiwan (Yu et al. 1997) and tectonic escape in southwestern Taiwan (Lacombe et al. 2001).

The northeasternmost South China Sea continental margin

Reflection seismic profiling of the Tainan Basin

Along the northeasternmost South China Sea continental margin, Tainan Basin is the dominant structure (Fig. 2). It is therefore one of our major targets of investigation for better understanding on the geology of northeasternmost South China Sea. Four seismic lines (973G, 973S1, 973S4 and E53) from three different sources were used in the study of basin stratigraphy and basement configurations. Acquisition parameters for these lines are listed in Table 1. Lines 973S4 and E53 are oriented subparallel to the continental margin while segment AB of line 973G is nearly perpendicular to lines 973S4 and E53 (Fig. 2). Figure 4 shows migrated multichannel seismic section ABC of line 973G, which passes through the part of Chinese continental shelf and slope where Tainan Basin is developed (Fig. 2). Following the notation of Lin et al. (2003), the Tainan Basin is subdivided into three NE-striking structures, named Northern Depression, Central Uplift, and Southern Depression, respectively (Figs. 2 and 4). It is striking to note immediately that across the Central Uplift seismic data show dramatically different stratigraphic characteristics and faulting styles.

Table 1 Acquisition parameters for seismic lines used in this study

Line names	973G	973S1 & 973S4	E53
Acquired by	GMGS*	SCSIO**	CNOOC***
Acquisition date	2001	2001	1989
Streamer channel	240	48	240
Record length (s)	10.024	12.0	5.0
Sampling rate (ms)	2	2	2
Receiver interval (m)	12.5	25.0	12.5
Shot interval (m)	50	50	25
Airgun volume ($inch^3$)	3,000	1,370 or 1,520	3,946

* GMGS: Guangzhou Marine Geological Survey, Chinese Ministry of Land and Resources

** SCSIO: South China Sea Institute of Oceanology, Chinese Academy of Sciences

*** CNOOC: China National Offshore Oil Corperation

In the Northern Depression, seismic data show mostly northwest-dipping normal faults cutting through almost the entire Cenozoic stratigraphy (Fig. 4). This signifies that these faults remained active until the late Cenozoic in primarily a weak extensional environment, accompanying gradual southeastward increase of thermal subsidence. Some of the larger faults can be traced down to the upper crustal basement and apparently control the basement structures. They often behave as growth faults bounding half-grabens in the Northern Depression.

Line 973G was designed to pass through two industrial wells, A1 and C1, within the Northern Depression (Figs. 2 and 4). Based on published data about these wells (Petroleum Geology of China, Vol. 16, 1990; Tzeng 1994) and unconformities identified on seismic section, we are able to correlate major stratigraphic boundaries on line 973G. Drilling data indicate that the basement rocks are generally Lower-to-middle Cretaceous sandstones with interbedded shales of shallow marine to continental environments (Wang et al. 2000a, b; Xia and Huang 2000; Feng et al. 2001; Lin et al. 2003). The top of the Mesozoic is marked by an unconformity representing a stratigraphic hiatus from the Upper Cretaceous to Lower Oligocene (Lee et al. 1993; Tzeng 1994; Lin et al. 2003). The existence of this unconformity indicates strong uplift and erosion during Cretaceous and Early Tertiary time. Unlike seismic data from most other sedimentary basins nearby, e.g., the Pearl River Mouth Basin to the southwest (Fig. 2; Clift and Lin 2001), Line 973G does not show clear synrift deposition within the Northern Depression. Synrift deposition normally appears as chaotic and wavy reflections of low frequencies at paleo-depocenters overlain with a break-up unconformity, but these reflective characteristics are not clearly present within the Northern Depression. Similar arguments have also been made based on studies from other seismic lines in this basin (Lee et al. 1993; Lin et al. 2003). Post-rift sediments in the Northern Depression are thin, upper Oligocene transgressive sandstones and thick younger marine shale (Lin et al. 2003). The Oligocene sequence is generally thin and limited to basin centers (Tzeng 1994). At well A1, the Oligocene was reported missing (Petroleum Geology of China, Vol. 16, 1990; Tzeng 1994), but on the northern flank of the half-graben located north of the Central Uplift well C1 may have reached Oligocene layers (Tzeng 1994).

While Cenozoic strata in the Northern Depression appear to be laterally continuous except for being faulted, they become chaotic, less continuous, and moderately deformed toward the southeast, especially

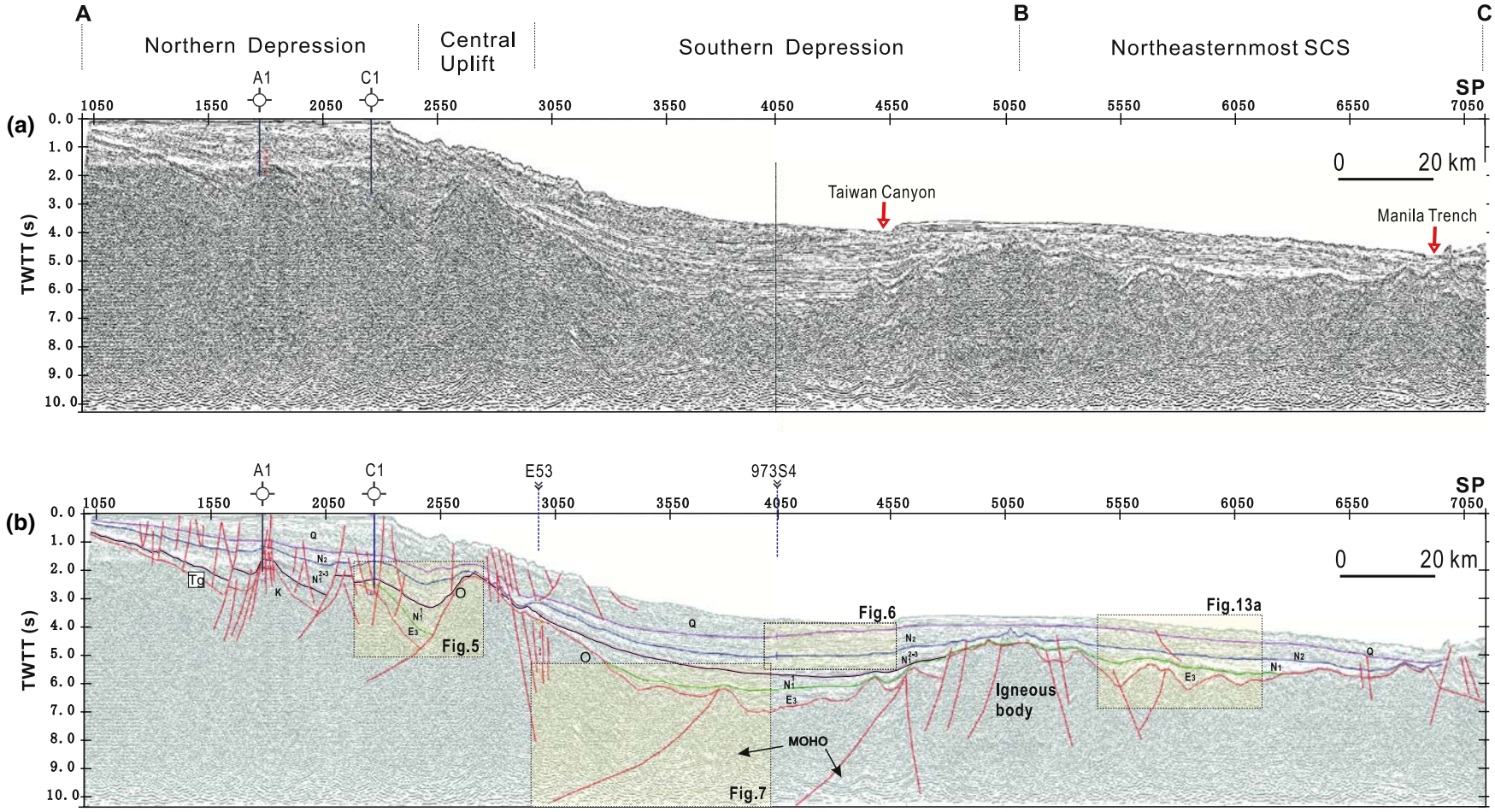
A
B
C
Northern Depression
Central Uplift
Southern Depression
Northeasternmost SCS
A1
C1
SP
(a)
TWTT (s)
0 20 km
Taiwan Canyon
Manila Trench
(b)
E53
973S4
Tg
K
Q
N2
O
E3
Fig.5
Fig.6
Fig.13a
Fig.7
Igneous body
MOHO

◀ Fig. 4 (**a**) Migrated seismic segment ABC of line 973G. (**b**) Geological interpretation. TWTT = two-way travel time; SP = shot point; O = onlap; Moho = Mohorovicic discontinuity. A1 and C1 are well names. E53 and 973S4 are two seismic lines intersecting line 973G. Locations of close-up views for later figures are also shown on panel (**b**)

in the proximity of the Central Uplift (Fig. 4). This characteristic change in reflections is caused by the presence of reef build-ups, rock type variations, and rock deformation near the present and past continental shelf breaks. High-angle normal faults are found above the southeast flank of the Central Uplift. These are active faults cutting through the uppermost sedimentary layers and deforming the sea bed into stepwise landforms, which indicate frequent shallow gravity collapses at this locality. It is also noted that the slope instabilities are accompanied by ocean bottom simulating reflectors. The landward flank of the Central Uplift is bounded by a northwest-dipping normal fault, which shows strong but sporadic seismic reflections and appears to penetrate the upper crust. To the northwest of the fault there is a half graben, in which lower Cenozoic sequences generally dip to the south at increasing dipping angles with depths (Fig. 5), showing a normal sense of movement along the fault.

From seismic stratigraphy analysis, three stages of vertical differential movement between the Central Uplift and the graben basement can be identified. The first stage corresponds to a rapid differential movement across the fault during the Oligocene, during which most of the sediments were derived from the northwest and sequence unit A was deposited (Fig. 5). At the start of the second stage, although the relative rate of

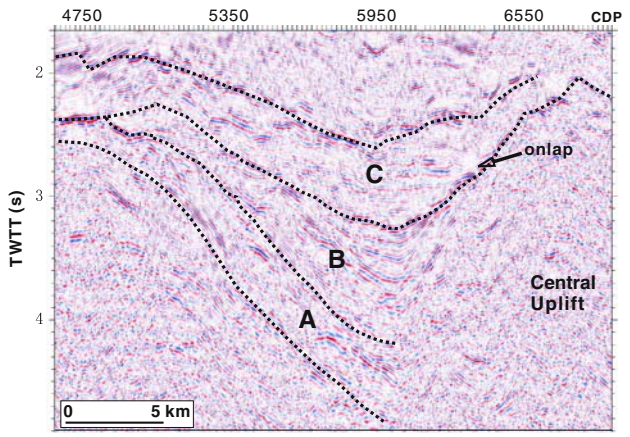

Fig. 5 Seismic facies A, B and C from the half graben indicating three stages of differential vertical movement between the Central Uplift and Northern Depression. Facies B (early Miocene) contains materials from the erosion of the Central Uplift. Onlaps to the Central Uplift in facies C (late Miocene) indicate progressive subsiding of the Central Uplift during the late Miocene. See Fig. 4(**b**) for location

uplift of the Central Uplift was diminished, erosion occurred there as it became subaerial. Source materials were carried to the graben from both the continent and the Central Uplift, and the lower Miocene sequence unit B was formed. In the third stage, the Central Uplift ceased its relative uplift and started to subside, probably during the late Miocene (Lee et al. 1993), and terrestrial sedimentary sequence C was deposited onlapping the Central Uplift and sequence B until the Central Uplift was buried.

Compared to the Northern Depression, the Southern Depression is still poorly understood, because so far petroleum exploration activities have almost been completely confined within the Northern Depression. Based on drilling data from the two wells in the Northern Depression, and from the Ocean Drilling Program (ODP) Site 1148 (Li et al. 2004) that is linked to line 973G by seismic profiles, we interpreted major stratigraphic boundaries in the Southern Depression, as shown in Fig. 4. Seismic reflections in the Southern Depression are drastically different from those of the Northern Depression. Deformation and faulting are scarce in the Cenozoic sedimentary layers in the Southern Depression, but the basement unconformity (Tg) beneath the Southern Depression is more readily identifiable. Additionally, the pre-Pliocene sequence in the Southern Depression is characterized as a fan-like unit with a good continuity of seismic reflections (Fig. 4). The lower Miocene and upper Oligocene sequences onlap onto the Central Uplift, and flatten and spread out to the southeast. The primary source of sediments was to the northwest, and the sea level may have remained relatively steady when Oligo-Miocene sediments were being deposited. The good lateral continuity of these sequences suggests a quiet and deep-water sedimentary environment, or a unique source of sediments, which might be the Central Uplift, which was a positive landform during the early Miocene and late Oligocene. For both scenarios it suggests that the Central Uplift was a longstanding positive feature, which served on the one hand as a source of sediments due to its erosion, and on the other hand as a blocking barrier between two distinct sedimentary environments.

Near the top of the Miocene unit, a marine downlap feature is observed to the southeast side of the Southern Depression (Fig. 6), and in the top unit directly above this marine downlap, a sequence showing obvious landward tapering is observed. These features indicate significant sedimentary environmental change near the Miocene–Pliocene boundary, which was concurrent with the end of erosion on the Central Uplift and with the onset of material influx from the southeast. Marine downlap features within similar

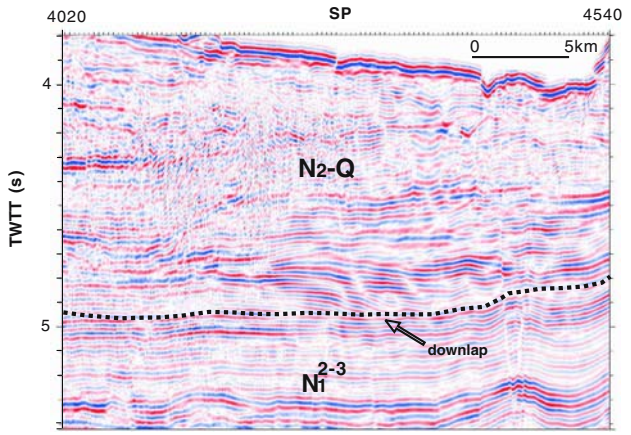

Fig. 6 Marine downlaps are observed in the Southern Depression near the interface (dotted line) between the Miocene and the Pliocene sequences. This feature implies significant changes in sedimentary environments and source material influx across the major unconformity. See Fig. 4(**b**) for location

sequences were also observed from a seismic line that is nearly parallel to, but to the northeast of ours (Chen and Jaw 1996), indicating a regional rather than local distribution. Seismic reflections from the Pliocene-Quaternary layers are less continuous within the Southern Depression, but can be traced laterally from the Southern to the Northern Depression. This suggests that after the late Miocene, the Central Uplift was no longer a topographic barrier between the Northern and Southern Depressions.

One important observation comes from the basement reflection beneath the Southern Depression (Fig. 7). A prominent landward dipping reflector of strong seismic amplitude is found separating two different tectonic blocks. The region adjacent to the reflector in the northwestern block shows primarily southeastward dipping seismic reflections, while seismic reflections in the southeastern block dip to the northwest, thus forming a sagging belt along the reflector. Strong but undulating reflections from the Moho in the southeastern block are clearly observable, which contrast with seismic reflections in the northwestern block.

Line E53 (Fig. 8) and line 973S4 (Fig. 9) provide additional constraints on the nature of crust across the strong crustal reflector. Line E53 intersects with line 973G at the southeastern flank of the Central Uplift (Fig. 4), where southeastward dipping reflections of the Central Uplift show good lateral continuity when viewed from line E53. From regional stratigraphic correlation, we infer that the Central Uplift at the intersection of E53 and 973S4 is likely composed of Upper Jurassic and Lower Cretaceous sedimentary rocks (Fig. 8). The first well (MZ1-1) drilled for the Mesozoic by Chinese National Offshore Oil Company (CNOOC) in 2003 revealed that Upper Jurassic and Lower Cretaceous rocks on the Dongsha Uplift are mainly sandstones and mudstones interbedded with basalt, rhyolite, and limestone.

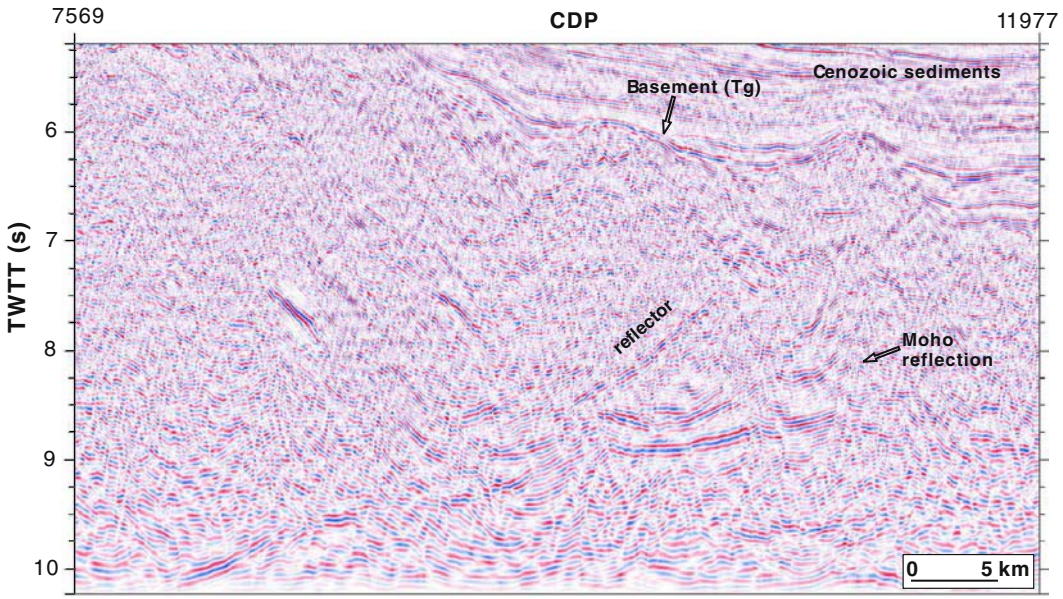

Fig. 7 Strong crustal seismic reflections within the basement beneath the Southern Depression show a convergent belt of thick continental crust to the northwest and thin oceanic or extended continental crust to the southeast. The dipping directions of seismic reflections change sharply across the reflector. Also noticeable is the elevated Moho reflections to the southeast of the reflector. CDP = common depth point

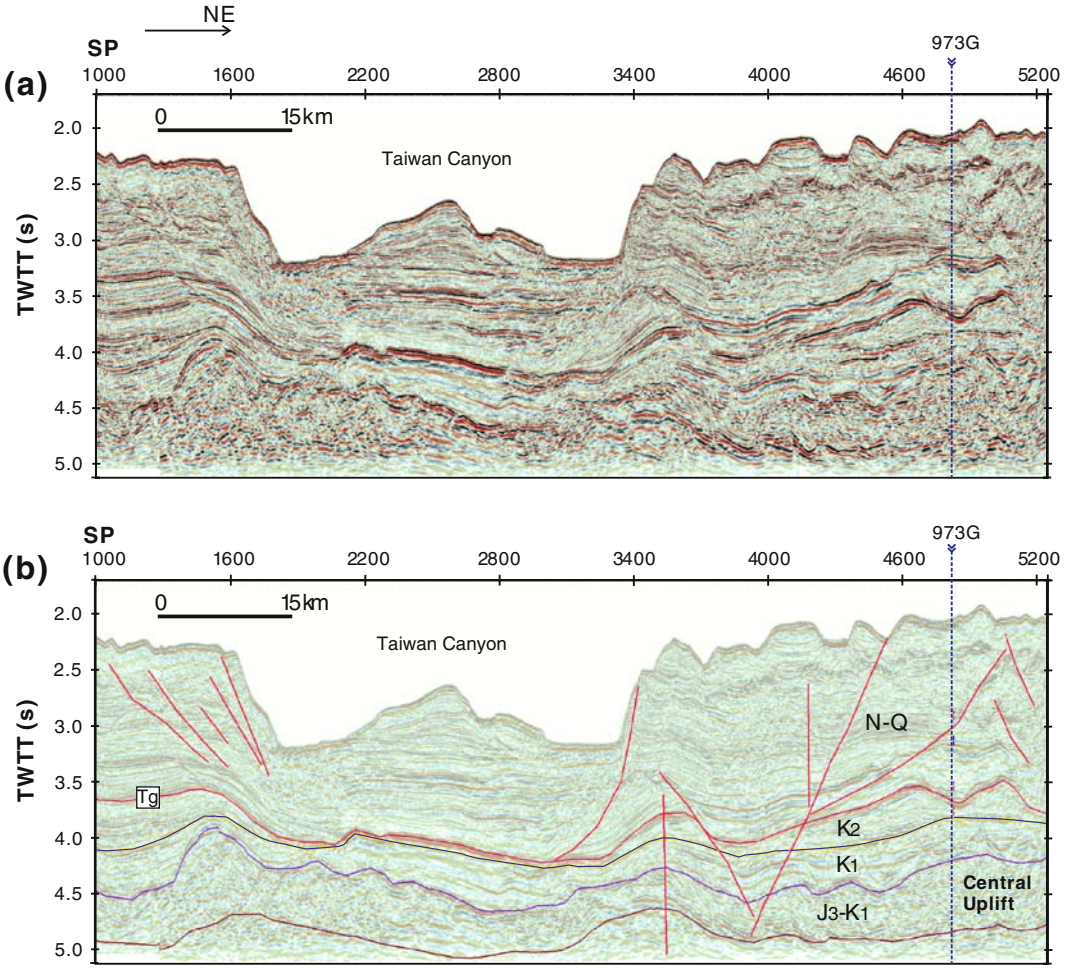

Fig. 8 Line E53 intersects with line 973G at the southern verge of the Central Uplift of the Tainan Basin. It can be observed that the shallow part of the Central Uplift might be composed of late Jurassic and early Cretaceous sedimentary rocks

To the south of the strong reflector, line 973S4 intersects with 973G within the central Southern Depression (Figs. 4 and 9). We note that on line 973S4 in the proximity of the Taiwan Canyon (Fig. 1), Cenozoic strata are consistently offset. Based on geophysical data within the northern South China Sea, Hsu et al. (1998) suggested that there is a relic transform fault located roughly along the Taiwan Canyon, which may mark the southwestern end of the former Ryukyu trench-arc system (Sibuet et al. 2002). Several sedimentary and structural differences across the suggested relic transform fault are also prominent on line 973S4, when examined in detail on a workstation. First, the Cenozoic reflections to the southwest of relic transform fault are of high frequency, wavy but continuous, while those to the northeast of the relic transform fault show relatively low frequency and lateral continuity. These differences may due to variations in lithology and/or sedimentary environments, or to different transport distances from the sediment sources for the two domains. Secondly, the Cenozoic basement (Tg) has a breakpoint near the relic transform fault (Fig. 10). To the southwest, Tg is easily identifiable, undulating locally, but taking an almost linear trend from the southwest to the northeast. In contrast, this basement trend makes a sharp turn at the breakpoint, taking a lower dipping gradient to the northeast in the central Southern Depression. Furthermore, to the northeast side of the relic transform fault Tg becomes less identifiable, with only minor local undulations. These differences argue for the existence of the proposed relic transform fault, across which there exist two different crustal domains. All the above observations, together with the significant depth of the basement (>9 km in depth and 7 s in two-way travel time) within the central Southern Depression, suggest that the part of the Southern Depression located south of the strong reflector and east of the relic transform fault comprises a basement of oceanic crust.

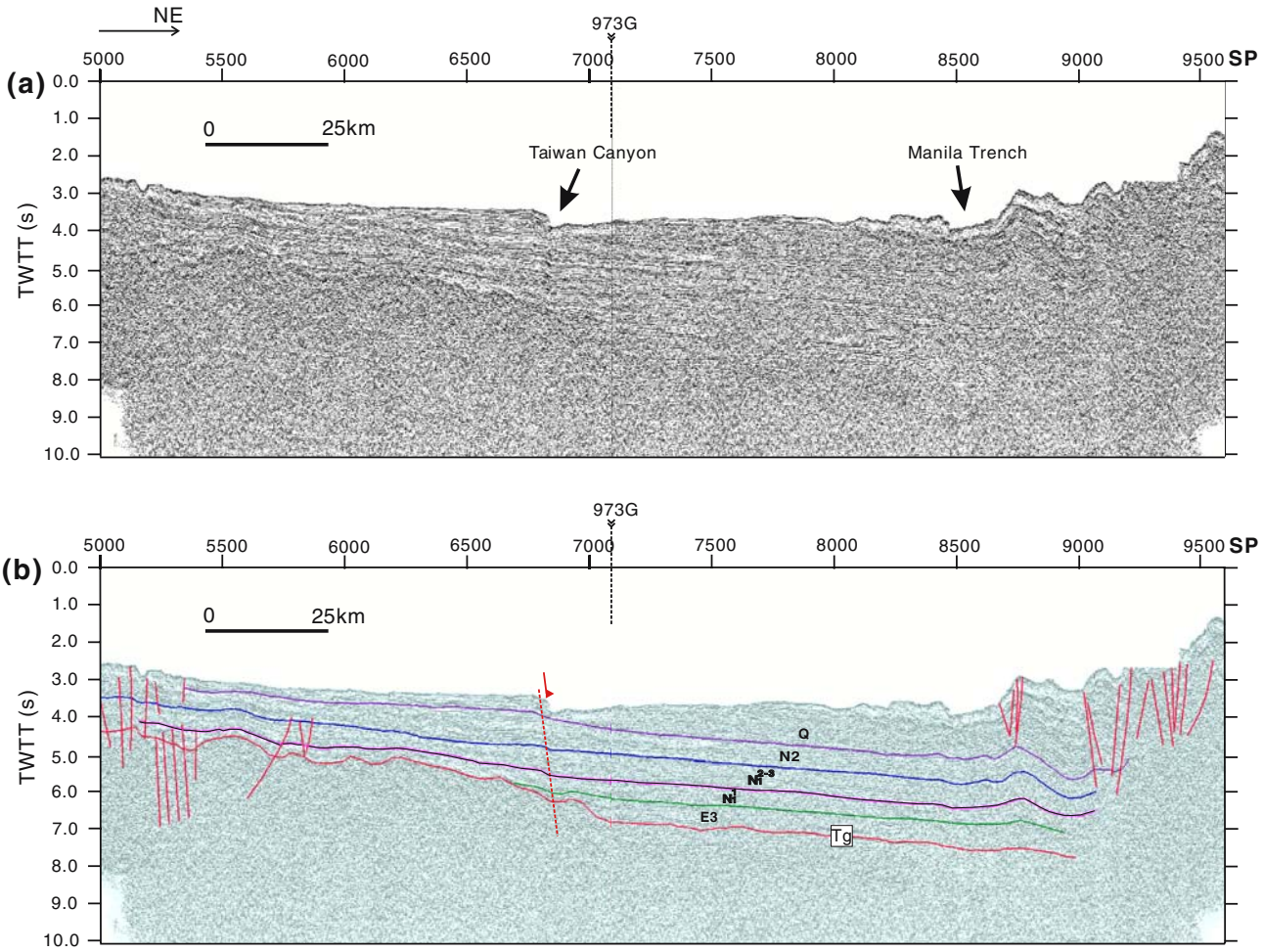

Fig. 9 (**a**) Line 973S4 (shotpoint number from 5,000 to 9,389) in the Tainan Basin area (upper panel), and its interpretation (**b**). Around the Taiwan Canyon, the Cenozoic sediments are consistently offset, which may indicate the existence of a relict transform fault (RTF). Furthermore, the seismic reflection characters change considerably across the RTF

Gravity modeling across the Tainan Basin

Gravity modeling can provide valuable insights on deep crustal structures and regional tectonic models. Free-air gravity anomalies are extracted along segment AB of line 973G from satellite-derived free-air gravity data of 2-min grid (Sandwell and Smith 1997). In our modeling we use the freeware version of GeoModel 2.01 written by Professor Gordon R. J. Cooper at University of the Witwatersrand, South Africa. This software performs simultaneous magnetic and gravimetric modeling using a Talwani-type algorithm (Talwani et al. 1959), with functionalities for inverting susceptibility, density, depth, width, and strike angle from observed anomalies. Because layer boundaries can be constrained by reflection seismic data, inversion helps in refining the density value for a given layer. We applied a simple model of four layers (water, sediment, crust and upper mantle), which nevertheless suffices to roughly constrain our results. Seafloor topography is calculated from seismic data, assuming a constant sea water velocity of 1.468 km/s, and basement depths are estimated based on the depth versus travel-time curve from well A1. The depths to the Moho beneath the Southern Depression are also estimated from seismic reflections.

Density logging on ODP Site 1148 obtained an average bulk density for the sediments at 1.884 g/cm^3, which is a very small number compared to the bulk density of sedimentary rocks (Wang et al. 2000a, b). It should be remembered that the Cenozoic sedimentary rocks recovered at ODP Site 1148 are loosely cemented and about 850 m thick. The much thicker sediments within Tainan Basin should have a higher average density than 1.884 g/cm^3. From well A1 it is known that the Cenozoic rocks are mostly sandstones and shale (Petroleum Geology of China, Vol. 16, 1990), which normally have dominant densities around 2.40

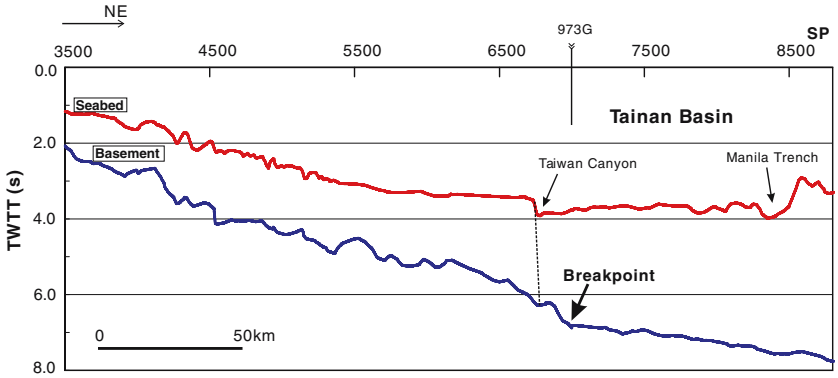

Fig. 10 Basement (Tg) configuration (interpreted from shotpoint number 3,500–8,800 from line 973S4) of the Tainan Basin showing a breakpoint on Tg around the interpreted relict transform fault (shown as a northeastern dipping dash line)

g/cm^3. Based on burial depths and lithologies, we take 2.40 g/cm^3 as the average density of sediments in gravity modeling. The density of the crustal layer is derived from earlier crustal structure studies in the region (e.g., Nissen et al. 1995a; Chen and Jaw 1996; Nakamura et al. 1998; Yan et al. 2001; Qiu et al. 2001), and we applied the Nafe-Drake curve (Ludwig et al. 1970) in the velocity–density conversions. The final density model from gravity modeling is shown in Fig. 11, from which two different crustal types can be instantly observed across the strong reflector. To the northwest the crustal thickness is up to 28 km, while to the southeast the crust is thin, less than 10 km beneath the Southern Depression, showing a significant landward increase in Moho depth. Thus both gravimetric and seismic data support a significant geological boundary along the strong reflector.

As observed beneath many other extensional continental margins, lower crustal layers of high seismic velocities at around 7.2 km/s have also been reported beneath the northern South China Sea continental margin (Yao et al. 1994; Nissen et al. 1995a; Kido et al. 2001). While it has been hypothesized that these layers might be underplated upper mantle materials during continental rifting (Kido et al. 2001), Nissen et al. (1995a) argued that high-velocity lower crustal materials beneath the South China Sea continental margin are due in larger part to variability in pre-rift crustal structure. Our gravity modeling shows that the high gravity anomalies on the continental margin may result from a shallow Moho and a thin crust (Fig. 11). Due to the non-uniqueness of the inversion calculation, one may equally argue that high gravity anomalies are caused by lower crustal underplating beneath the continental crust, though we did not intend to model possible underplating. The crustal thickness beneath the Central Uplift is large, suggesting that it is a deeply rooted feature.

The northeasternmost South China Sea basin

To the south of Tainan Basin is the northeasternmost South China Sea basin. Recent geophysical studies in this area include reflection seismic, gravimetric and magnetic surveys, ocean-bottom seismograph (OBS) experiments, bathymetric sounding, and earthquake hypocenter relocations (Xia et al. 1994; Chen and Jaw 1996; Wu et al. 1997; Cheng et al. 1998; Hsu et al. 1998;

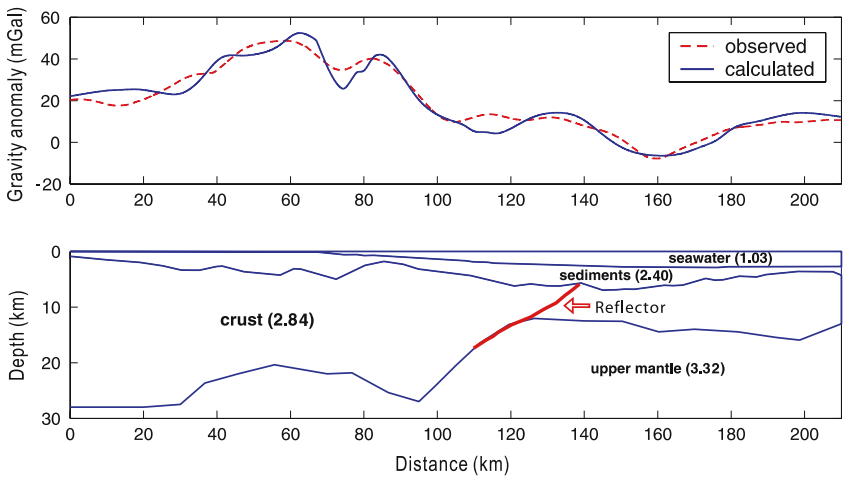

Fig. 11 Gravitational modeling/inversion with a 4-layer depth model with densities (g/cm^3) shown in parentheses

Nakamura et al. 1998; Kao et al. 2000; Tang and Chemenda 2000; Wang et al. 2000a, b; Bautista et al. 2001; Huang et al. 2001; Chi 2003). In 1987, SCSIO obtained an early 24-channel seismic reflection transect (Xia et al. 1994; Wang et al. 2000a, b; Huang et al. 2001), which is located close to Line 973G. Chi (2003) investigated the tectonic wedging along the rear of the Hengchun Ridge (Fig. 2) based on seismic and gravity data. Hsu et al. (1998) updated the free-air gravity anomaly and magnetic anomaly maps around Taiwan by incorporating newly obtained datasets. Crustal thicknesses revealed from OBS experiments west of the Hengchun Peninsula and Manila Trench indicated a progressive southeastward crustal thinning from an extended continental crust of 11 km thick to an oceanic crust of 5–6 km thick (Chen and Jaw 1996; Nakamura et al. 1998). A number of earthquake hypocenter relocations and tomographic studies help with delineating the subduction of the South China Sea plate beneath the Philippine Sea plate, the Eurasian continental subduction beneath the Taiwan orogen, as well as the transition from a subduction to a collision southeastern Taiwan (Wu et al. 1997; Cheng et al. 1998; Kao et al. 2000; Tang and Chemenda 2000; Bautista et al. 2001).

With relatively quiet magnetic anomalies of long-wavelengths (Fig. 3), the northeastern part of the South China Sea distinguishes itself from other parts of that basin. Many have postulated that its crustal origin and age might be different from other parts of the South China Sea basin (Sibuet and Hsu 1997; Sibuet et al. 2002, 2004; Pautot et al. 1986). Xia et al. (1997) found a lower crustal Vp/Vs ratio of 1.87–1.96 for this region, and they characterized this ratio to be of a paleo-oceanic crust. Line 973G can help provide new constraints on such speculations. Figs. 4 and 12 show the segment of line 973G that passes through the northeastern part of the South China Sea. It can be observed from Fig. 12 that water depths increase stepwise, from about 3,000 m in South China Sea basin,

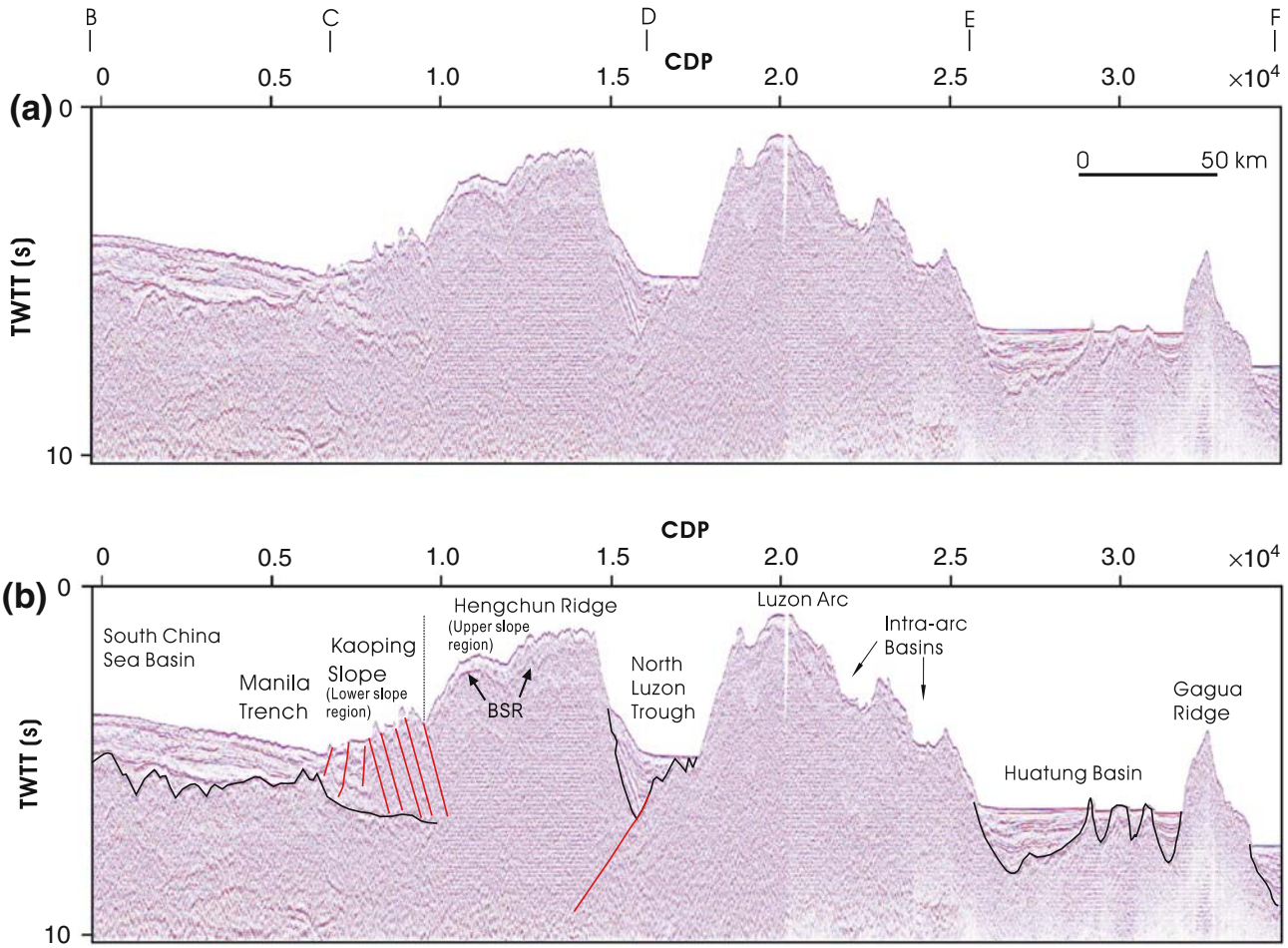

Fig. 12 (**a**) The migrated seismic section along segment BCDEF of line 973G. (**b**) Preliminary geological interpretations of faults and sedimentary basement. TWTT = two-way travel time; CDP = common depth point; BSR = bottom simulation reflector

to about 3,600 m in the northern Luzon Trough, about 4,760 m within the Huatung Basin, and about 5,550 m east of the Gagua Ridge. Li et al. (2007, in press) have shown that the northeasternmost South China Sea has significantly lower Bouguer gravity anomalies and lithospheric densities than Huatung Basin.

Immediately to the south of the Southern Depression is an intrusive igneous body bounded on both sides by faults. The presence of igneous bodies to the south of the Southern Depression is also evident on line 45 of Sibuet et al. (2002). On line 973G this igneous body is situated to the southwest of the proposed relict transform fault. Upper Oligocene strata appear to be absent on the top of the igneous body, but they are present within the Southern Depression to the north and within small depressions to the east. The basement (Tg) to the east of the igneous body is apparently folded (Fig. 13a), and beneath Tg, folded reflections subparallel to Tg are also clearly present. These folded reflections within the northeasternmost South China Sea basement might be caused by Mesozoic layers subjected to an early phase of faulting, and they are sharply different to chaotic but unfolded reflections from the central South China Sea basement (Fig. 13b). Above Tg, Cenozoic sequences lie uncomfortably on the basement and post-Oligocene strata are only slightly tilted toward the Manila Trench.

To summarize, we find that the northeasternmost South China Sea differs from the central South China Sea in terms of seismic reflections. While the central South China Sea is formed by Oligocene–Miocene oceanic floor spreading, the northeasternmost South China Sea appear to be accompanied by a more complicated geological history. The northeasternmost South China Sea may comprise paleo-oceanic crust on which Mesozoic sediments were deposited and later deformed. Seismic reflection differences indicate that the northeastern South China Sea might be older than the central South China Sea. However, the basement within the central South China Sea is substantially deeper (Fig. 13). We cannot rule out that the northeastern South China Sea is underlain by a heavily extended continental crust showing mild magnetic anomalies. The folds in the basement may be the result of a phase of deformation, caused either by the late Mesozoic paleo-Pacific plate subduction, by an early Cenozoic Ryukyu subduction, or by continental rifting and drifting. Nevertheless, the northeastern-

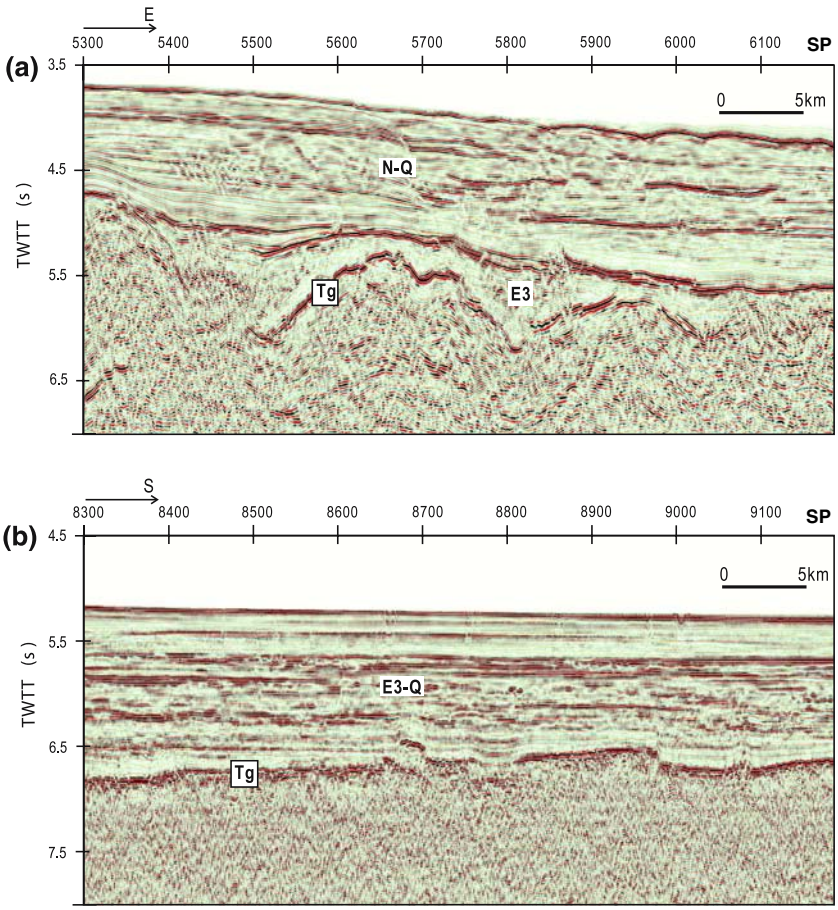

Fig. 13 Comparison between seismic reflections from line 973G in the northeasternmost South China Sea (**a**) and from line 973S1 in central South China Sea (**b**). See Figs. 2 and 4(**b**) for line locations

most South China Sea crust appears to be more complicated than simple oceanic or extended continental crust. We have already observed the differences across the relict transform fault. In addition, the Southern Depression of the Tainan Basin shows several lines of evidence that it is partially underlain by oceanic crust. Crustal thicknesses of this region assessed by many geophysical studies range anywhere from 11 km to 5–6 km (Chen and Jaw 1996; Nakamura et al. 1998).

Discussion

The crustal seismic reflector

Strong crustal and mantle seismic reflectors have been observed in many parts of the world (Jones and Nur 1984; Warner et al. 1996). Along the northern South China Sea continental margin, landward-dipping crustal reflectors (Fig. 1 for locations) cutting through the entire crust have also been identified from multichannel reflection seismic surveys (Yao et al. 1994; Nissen et al. 1995b; Hayes et al. 1995). These reflectors have been tentatively postulated as being developed along the late Mesozoic paleo-Pacific plate subduction (Yao et al. 1994), and they may represent Cenozoic throughgoing crustal faults where extensive crustal thinning has occurred (Nissen et al. 1995b; Hayes et al. 1995). Furthermore, crustal velocity structures derived from two-ship expanding spread profiles show abrupt changes across the Xisha Trough where a Mesozoic suture zone has been proposed (Yao et al. 1994; Nissen et al. 1995b), despite the fact that a study based on ocean bottom seismometers on a nearby traverse implied similar crustal structures on both sides of the Xisha Trough (Qiu et al. 2001). The strong crustal reflector identified on line 973G presents itself as an interesting and important feature. It has a dip angle of about 18°. The reflector exists only in the basement, beneath the Cenozoic sedimentary cover of the Southern Depression, serving a sharp dipping boundary between the northwestern continental block and the southeastern oceanic or attenuated continental crust.

In one possible scenario, we suggest that line 973G reveals a buried subduction zone beneath Cenozoic sedimentary layers. The Southern Depression could initially be a relict trench where the bottom unit was deposited primarily in a deep-water environment. If this was a trench, the southeastern half of the Southern Depression would then be expected to be underlain by oceanic crust, consistent with our earlier analyses. The Northern Depression appears to be located between an accretionary prism (the Central Uplift) and a volcanic arc, which shows up as a strong positive magnetic anomaly belt laying nearly parallel to the continental margin (Fig. 3). Assuming that the proposed subduction is real, its geological evolution remains unclear. It has long been suggested that a Mesozoic subduction zone existed along the offshore coastal region of south China (Jahn et al. 1976; Hamilton 1979; Gilder et al. 1996; Zhou et al. 1996; Lapierre et al. 1997; Chen and Jahn 1998; Zhou and Li 2000), but its exact location has remained as a focus of argument because complex Cenozoic tectonic events have completely altered the Mesozoic configuration. Instead of being an active subduction zone, the present-day southern China continental margin (Fig. 1) to the southwest of Taiwan is passive, and has evolved from the continental break-up and subsequent seafloor spreading of the South China Sea (Taylor and Hayes 1980, 1983; Holloway 1982). At the same time to the northeast of Taiwan, the active Ryukyu Trench is associated with subduction of the western Philippine Sea plate, rather with the subduction of the suggested Mesozoic paleo-Pacific plate. This Cenozoic transformation on Mesozoic tectonics presents itself as a major hurdle to understanding the Mesozoic evolutionary history of this region. Developed immediately to the north of the Tainan Basin as a positive magnetic belt, the offshore South China Magnetic Anomaly (SCMA) (Fig. 3) lines up along the continental margins and trends parallel to the coast and to regional tectonic trends. The SCMA does not appear to extend over the continent-ocean transition zone based on the studies of numerous seismic lines, but exists primarily on the continental shelf. It is thus unlikely to be associated with Cenozoic magmatism concomitant with continental rifting and opening of the South China Sea. The nearly north-south opening of the eastern South China Sea sub-basin causes the magnetic anomaly belts to lie in a west–east direction, which is disconcordant with the strike of the NE-trending SCMA. This indicates that the eastern South China Sea sub-basin and the SCMA are not congenetic. Furthermore, the SCMA shows signs of deformation by Cenozoic tectonic activities. The SCMA magnetic belt is intercepted by the Taiwan orogen to the northeast and is cut by the Xisha Trough and the South China Sea basin to the southwest. A Mesozoic age for the SCMA is in line with other suggestions that the SCMA reflects a buried Mesozoic volcanic arc from paleo-Pacific subduction (Yao et al. 1994), and is also consistent with the interpretation that the region of strong crustal reflection on line 973G may have well been the site of a Mesozoic subduction zone. This

hypothesis is further supported by crustal density structures from gravity modeling presented in this paper and by the presence of deformed basement seismic reflections near the strong crustal reflector. Alternatively, the proposed subduction might be Cenozoic. Sibuet and Hsu (1997) identified four belts of basins and associated ridges on the Chinese continental shelf and classified them as relict back-arc basins and arcs of the Ryukyu subduction system that become successively younger seaward since the Early Tertiary. In their interpretations, the Northern Depression of the Tainan Basin was active during Oligocene and early Miocene rifting. During the early middle Miocene the suggested Ryukyu subduction zone in the area of the Southern Depression became inactive. Using two nearby seismic lines parallel to line 973G (see lines 45 and 34 on Fig. 2), Sibuet et al. (2002, 2004) interpreted a layer of deformed sediments in the basement as an old accretionary prism, and a body devoid of seismic reflections beneath the upper continental margin as a former volcanic arc. Although they did not identify strong reflectors as we present here, they concluded that there was an extinct northwestward dipping subduction zone beneath the Tainan Basin. Their study suggests that the geological structures we interpreted are not isolated features but extend to the northeast in a strike nearly parallel to the present-day coastline.

In a second possible scenario, the reflector might also be related to Early Cenozoic continental extension, comparable to the S-reflector west of Galicia (Reston et al. 1996). Our seismic stratigraphic analyses indicate Oligocene vertical differential movement between the Northern Depression and Central Uplift, and slightly later erosion on the Central Uplift, suggesting active uplift of the Central Uplift in the Miocene. The Central Uplift probably remained as a positive feature from the Late Cretaceous to the Late Miocene. Several major northwestward-dipping faults within the Northern Depression penetrated the basement, showing strong control on the basement topography, and forming at least four half-grabens. These major faults may also be explained by Oligocene continental rifting (Lee et al. 1993; Tzeng 1994) concurrent to the opening of the South China Sea. By the same reasoning, the strong crustal reflector, subparallel to the afore-mentioned major faults, may represent the point of continental break-up. The basement of the Southern Depression has an overall trough structure that might be related to continental rifting. To the southwest, the trough structure is truncated by the relic transform fault roughly along the Taiwan Canyon (Fig. 1).

Regional tectonics

Despite extensive geological studies in the region, some of the fundamental questions concerning the style and mechanism of the opening of the South China Sea remain unanswered. One of the open questions is how Cenozoic rifting followed Mesozoic subduction, or in what fashion did the presumed weak subduction zone control the Cenozoic rifting. Continental rifting along ancient suture zones has been observed in many other places around the world. For example, Mesozoic continental break-up along the North American–North African Atlantic margins followed the trend of the late Paleozoic Appalachian fold and thrust belt (Wilson 1966; Tommasi and Vauchez 2001; Harry and Huerta 2002), and intracontinental extension along the Baikal rift zone exploited the Paleozoic suture zone between the Archean Siberian Craton and the Caledonian–Hercynian fold belt (Delvaux et al. 1995, 1997; Lesne et al. 2000). Early stage of continental rifting in the South China Sea area may have also explored a late Mesozoic paleo-Pacific subduction zone developed in the South China Sea area (Jahn et al. 1976; Hamilton 1979; Gilder et al. 1996; Zhou et al. 1996; Lapierre et al. 1997; Chen and Jahn 1998; Zhou and Li 2000).

Tectonic transitions have been very common in western Pacific marginal seas (Li 2004). The Philippine Sea basin offers a vivid example of where transitions from transform fault to subduction zone and from subduction zones to spreading centers occur. Within the South China Sea basin, eastward subduction along the Manila Trench could be regarded as having initiated along a transform fault of the proto-South China Sea (Figs. 14 and 15). Following the same reasoning, it is not unnecessary to expect a logical genetic relationship between Cenozoic rifting and Mesozoic subduction along the northern South China Sea continental margin.

Another open question concerns two groups of tectonic reconstructions on whether the present-day South China Sea basin experienced primarily a single episode (e.g., Pautot et al. 1986; Hayes and Nissen 2005) or multiple episodes of extension and seafloor spreading (e.g., Ru and Pigott 1986; Yao et al. 1994). We favor multiple episodes of extension and seafloor spreading for the opening of South China Sea, based on increasing lines of evidence for sharp tectonic differences between the eastern and western part of the South China Sea region. The Zhongnan Fault (Fig. 1), characterized by a topographic high on the bathymetric map and by a magnetic anomaly boundary on the magnetic map (Fig. 3), bisects the South China Sea region. Across the Zhongnan Fault (Figs. 14 and 15),

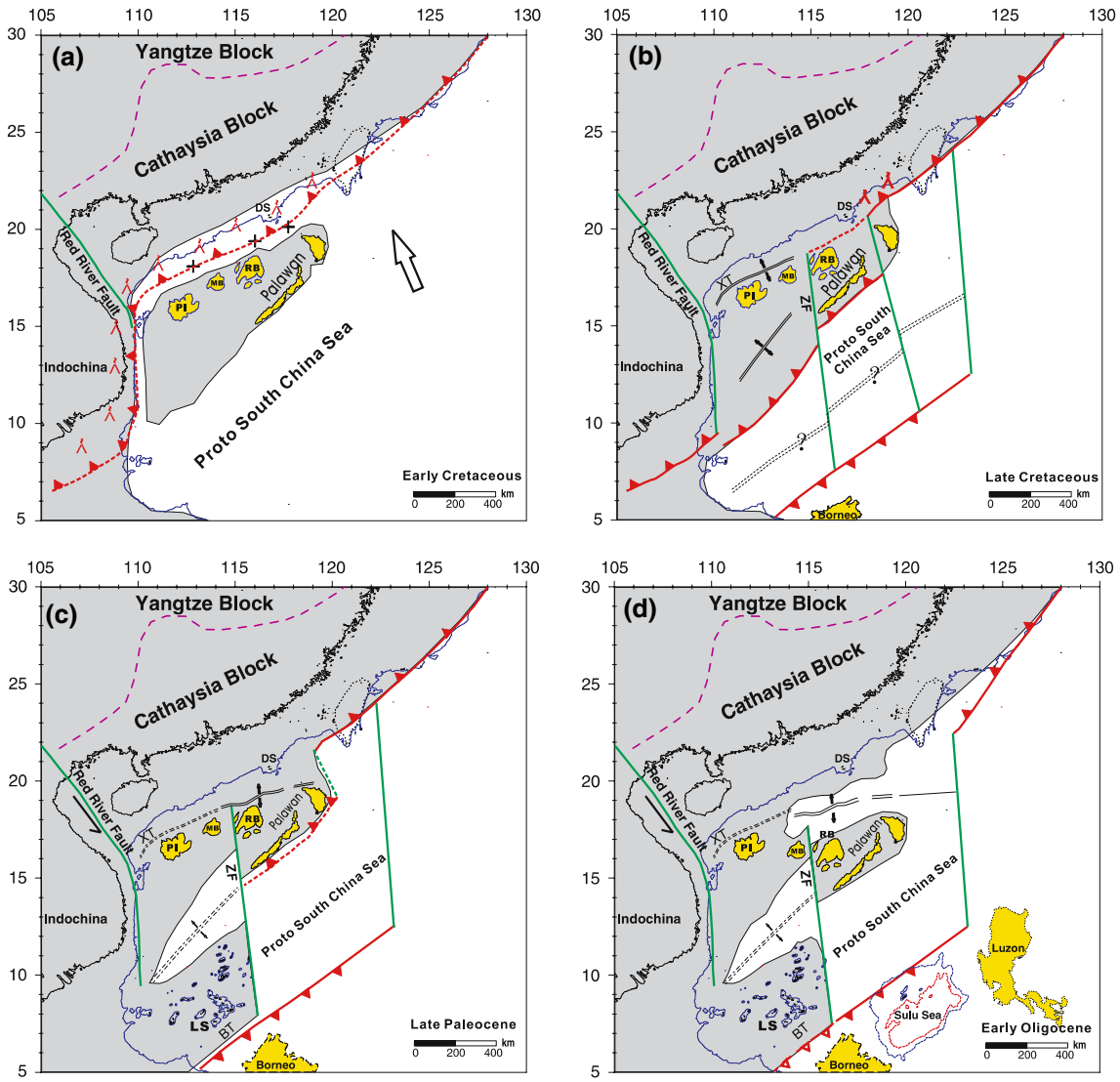

Fig. 14 Tectonic reconstruction of the South China Sea from the early Cretaceous to early Oligocene. The strike slip sense along the Red River Fault is determined from Leloup et al. (2001) and Clift and Sun (2006). See Fig. 15 for explanations

geological and geophysical differences are readily recognizable.

On the northern South China Sea continental margin, high velocity lower crustal materials appear to be more prominent to the northeast along the margin, while the total intensity of the South China Sea magnetic anomaly belt reduces to the southwest. These west–east differences may reflect lateral strength variations of an earlier Mesozoic subduction zone and diverse degrees of later alterations by Cenozoic rifting and drifting. We suggest that long-lived subduction created a weak crust, characterized by deep crustal faulting, mantle foliation and anisotropy, which could then facilitate continental rifting (Tommasi and Vauchez 2001).

Within the South China Sea basin, magnetic anomalies show sharp differences across the Zhongnan Fault, as demonstrated earlier. These differ not only in the strike of the magnetic belt, but also in planar magnetic patterns (Fig. 3). Yao et al. (1996) also noted from bathymetric studies that the western sub-basin is deeper than the eastern sub-basin by about 200 m on average. Age estimates from both bathymetric and magnetic data indicated that the western sub-basin could be formed about 10 m.y. earlier than the eastern sub-basin (Ru and Pigott 1986; Yao et al. 1994). In addition, while the relict spreading center in the western sub-basin is associated with a bathymetric and gravimetric low, it is shown as a topographic and gravimetric high in the eastern sub-basin. Collectively

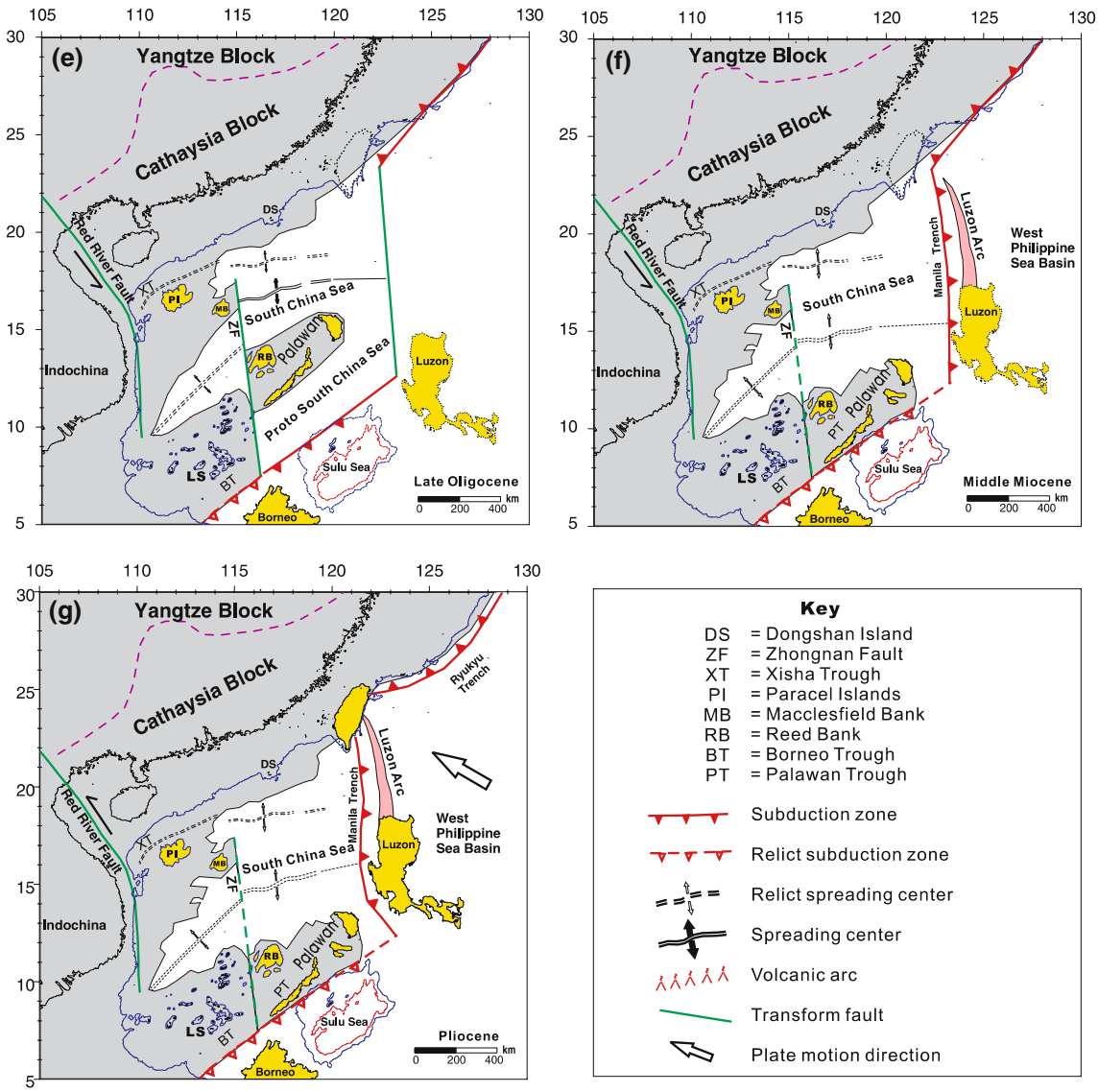

Fig. 15 Tectonic reconstruction of the South China Sea from the early Oligocene to Pliocene. The strike slip sense along the Red River Fault is determined from Leloup et al. (2001) and Clift and Sun (2006)

all these west–east differences argue in favor of an episodic opening model of the South China Sea basin (Figs. 14 and 15).

In our reconstruction (Figs. 14 and 15), neither significant continental rifting nor seafloor spreading occurred in the northeasternmost South China Sea, a model which is in agreement with Pautot et al. (1986) who stated that the eastern sub-basin probably formed in an area already floored by oceanic crust. This ancient piece of oceanic crust may have been part of the proto-South China Sea, a small fragment of the Mesozoic paleo-Pacific plate. With the opening of South China Sea, the major part of the proto-South China Sea was subducted southeastward and eastward along surrounding subduction zones. With coincident continental rifting and seafloor spreading of South China Sea, erosion occurred for the most part on the Chinese continental margin from the late Mesozoic to early Miocene (Lin et al. 2003). This reconstruction honors the afore-mentioned suggestion that there might be a long-lived relict of a proto-South China Sea. In conclusion, the opening of South China Sea may be attributed to interactions of multiple processes within a complex geodynamic system. Hypothesized eastward mantle extrusion caused by Tethyan closure (Flower et al. 2001), and the extrusion tectonics from India–Eurasian collision (Tapponnier et al. 1982), could have facilitated back-arc opening and eastward retreat of paleo-Pacific subduction zone. Southeastward mantle dragging on the

base of the proto-South China Sea plate may have jointly worked with the slab pull of the subducting proto-South China Sea plate to drive extension. Another feature of our reconstruction is that southeastward migration of late Mesozoic subducting systems results in relic trenches and back-arc basins as weak zones fostering Cenozoic extension and seafloor spreading, to which newly formed subducting systems to the southeast, however transient, may have initially imposed driving forces. One notable exception to the episodic rifting model is that of Briais et al. (1993), who suggested that the opening of eastern sub-basin predated that of the western sub-basin.

Conclusions

Some major northwestward-dipping faults have controlled the basement configuration of the Northern Depression, forming several half-grabens. The Tainan Basin area was exposed to a long period of erosion before Oligocene rifting. Late Oligocene sequences can be found mainly in the paleo-depocenters, such as one north of the Central Uplift. Vertical differential movement between the Northern Depression and Central Uplift continued from the late Oligocene to the late Miocene. The Central Uplift experienced episodic uplift and erosion, and worked as a topographic barrier between two different depositional environments before the Pliocene. The pre-Pliocene sedimentary sequences in the Northern Depression appear to be mostly terrestrial and show land and shallow marine sedimentary environments, while that in the Southern Depression came partially from the Central Uplift and deposited fine grained sediment in a deep water environment. Starting from the late Miocene, the area experienced continued thermal subsidence until the Central Uplift was buried.

Beneath the Southern Depression of the Tainan Basin there is a landward-dipping seismic reflector, which we interpret as a deep crustal fault forming a sharp boundary between continental crust and oceanic crust (or heavily extended continental crust). The Southern Depression is overall a trough structure, in which sediments with little deformation were deposited. The Southern Depression is bounded to the north by the Central Uplift and to the south by igneous bodies. On a seismic line subparallel to the continental margin, a sharp breakpoint is observed in the Southern Depression basement near the Taiwan Canyon, where a relict transform fault is also interpreted. This transform fault separates two blocks of slightly different magnetic patterns and basement depths.

Gravitational modeling supports the thinning of the crust southeast of the deep crustal reflector, and reveals a sharp landward increase in Moho depths to the north of the reflector. While the positive gravity anomaly observed near the continental break is probably caused by a shallow mantle or by magmatic underplating associated with Cenozoic continental rifting, the nearby offshore South China Magnetic Anomaly appears to be caused by shallow intrusive or extrusive magnetic sources located further to the north.

On Line 973G the northeasternmost South China Sea basin shows folded basement reflections, which are not like those seen in the central South China Sea basin and that were formed by seafloor spreading. This suggests that the northeasternmost South China Sea basin might be either older oceanic crust or strongly attenuated continental crust. However the existence of the Southern Depression and the transform fault may argue for the northeasternmost South China Sea basin itself not being a single geological unit. The Southern Depression in particular may be partially underlain by a sliver of oceanic crust, based on seismic reflection and gravity observations. Magmatic bodies are frequently observed on the southern edge of the Southern Depression. In addition, the northeasternmost South China Sea also sharply differs from the Huatung Basin to the east of the Luzon Arc, in terms of seismic reflections, water depths, and Bouguer gravity anomalies.

Regional geological and geophysical data, particularly the magnetic distribution, support an episodic opening model of the South China Sea. This model takes account of recent findings about Mesozoic distributions from drilling wells and seismic surveys, and honors our observations.

Acknowledgements Seismic data 973G were acquired by GMGS using vessel ''Tanbo'', and lines 973S1 and 973S4 were acquired with vessel ''Experiment-2'' by SCSIO. We thank the officers and crew of these vessels for their contributions. Appreciations go to Profs. Bochu Yao and Liaoliang Wang of GMGS, to Prof. Di Zhou of SCSIO, and to Profs. Huanjiang Chen, Jialin Wang, and Bing Chen of Tongji University for helpful discussions. GMT (Wessel and Smith 1995), and Seismic Unix (CWP, Colorado School of Mines) were used in data manipulation. Suggestions from two anonymous reviewers improved the readability. Additionally, we wish to extend our sincere gratitude to editors, P. Clift and Y. J. Chen, for their detailed review and numerous critical comments, which made the publication of this work possible. This research is funded by Chinese Natural Science Foundation (Grants 40504016 and 40321603), by Chinese Fundamental Research and Development Program (Grants G2000047604 and G2000078501), and by Nanhai East Institute of CNOOC Research Center.

References

Bautista BC, Bautista MLP, Oike K, Wu FT, Punongbayan RS (2001) A new insight on the geometry of subducting slabs in northern Luzon, Philippines. Tectonophysics 339:279–310

Briais A, Patriat P, Tapponnier P (1993) Updated interpretation of magnetic anomalies and seafloor spreading stages in the South China Sea: implications for the tertiary tectonics of Southeast Asia. J Geophys Res 98:6299–6328

Chemenda AI, Yang R-K, Stephan J-F, Konstantinovskaya EA, Ivanov GM (2001) New results from physical modeling of arc-continent collision in Taiwan: evolutionary model. Tectonophysics 333:159–178

Chen AT, Jaw Y-S (1996) Velocity structure near the northern Manila Trench: an OBS reflection study. Terr Atmos Ocean Sci 7:277–297

Chen JF, Jahn BM (1998) Crustal evolution of southeastern China: Nd and Sr isotopic evidence. Tectonophysics 284:101–133

Cheng W-B, Wang C, Shyu C-T, Shin T-C (1998) A three-dimensional Vp model of the southeastern Taiwan area and its tectonic implications. Terr Atmos Ocean Sci 9:425–452

Chi W-C (2003) From Subduction to Collision: Results from Seismic Profiling, Gravity Modeling, and Earthquake Finite Fault Inversions in Taiwan Region. Dissertation, University of California

Clift P, Lin J (2001) Preferential mantle lithospheric extension under the South China margin. Mar Petrol Geol 18:929–945

Clift P, Lin J, Barckhausen U (2002) Evidence of low flexural rigidity and low viscosity lower continental crust during continental break-up in the South China Sea. Mar Petrol Geol 19:951–970

Clift P, Schouten H, Draut AE (2003) A general model of arc-continent collision and subduction polarity reversal from Taiwan and the Irish Caledonides. In: Larter RD, Leat PT (eds) Intra-Oceanic Subduction Systems; Tectonic and Magmatic Processes. Geol Soc Spec Publ 219:81–98

Clift P, Sun Z (2006) The sedimentary and tectonic evolution of the Yinggehai-Song Hong Basin and the southern Hainan margin, South China Sea; implications for Tibetan uplift and monsoon intensification. J Geophys Res 111, DOI:10.1029/2005JB004048

Davis D, Suppe J, Dahlen FA (1983) Mechanisms of fold-and-thrust belts and accretionary wedges. J Geophys Res 88:1153–1172

Delvaux D, Moeys R, Stapel G, Melnikov A, Ermikov V (1995) Paleostress reconstructions and geodynamics of the Baikal region, Central Asia, I, Paleozoic and Mesozoic pre-rift evolution. Tectonophysics 252:61–101

Delvaux D, Moeys R, Stapel G, Petit C, Levi K, Miroshnichenko A, Ruzhich V, Sankov V (1997) Paleostress reconstructions and geodynamics of the Baikal region, Central Asia, II, Cenozoic rifting. Tectonophysics 282:1–38

Deschamps A, Monié P, Lallemand SE, Hsu S-K, Yeh KY (2000) Evidence for early Cretaceous oceanic crust trapped in the Philippine Sea plate. Earth Planet Sci Lett 179:503–516

Deschamps AE, Lallemand SE, Collot J-Y (1998) A detailed study of the Gagua Ridge: a fracture zone uplifted during a plate reorganisation in the Mid-Eocene. Mar Geophys Res 20:403–423

Editorial committee of Petroleum Geology of China (eds) (1990) Oil and Gas Bearing Areas on the Continental Shelf and its Neighbouring Regions. Vol. 16(1), Petroleum Industry Press, Beijing (in Chinese)

Feng X, Zhang C, Wang C, Gao L (2001) Mesozoic in the Eastern China Sea shelf and Taixinan Basin and its petroleum potential. China Offshore Oil Gas (Geol) 15:306–310 (in Chinese)

Flower MFJ, Russo RM, Tamaki K, Hoang N (2001) Mantle contamination and the Izu-Bonin-Mariana (IBM) 'high-tide mark': evidence for mantle extrusion caused by Tethyan closure. Tectonophysics 333:9–34

Geological Survey of Japan and Coordinating Committee for Coastal and Offshore Geoscience Programmes in East and Southeast Asia (CCOP) (1996) Magnetic anomaly map of East Asia 1:4,000,000 CD-ROM Version, Digital Geoscience Map 2 (P-1)

Gilder SA, Gill JA, Coe RS, Zhao X, Liu Z, Wang G, Yuan K, Liu W, Kuang G, Wu H (1996) Isotopic and paleomagnetic constraints on the Mesozoic tectonic evolution of south China. J Geophys Res 101:16137–16154

Hall R (2002) Cenozoic geological and plate tectonic evolution of SE Asia and the SW Pacific: computer-based reconstructions, model and animations. J Asian Earth Sci 20:353–431

Hall R, Ali JR, Anderson CD Baker SJ (1995) Origin and motion history of the Philippine Sea Plate. Tectonophysics 251:229–250

Hamilton W (1979) Tectonics of the Indonesian region. USGeol Surv Prof Pap 1078:345

Harry DL, Huerta AD (2002) Wilson Cycles, tectonic inheritance, and rifting of the U.S. Atlantic and Gulf of Mexico margins. Geol Soc Am Abs Prog 34(6):21

Hayes DE, Nissen S, Buhl P, Diebold J, Yao B, Zeng W, Chen Y (1995) Through-going crustal faults along the northern margin of the South China Sea and their role in crustal extension. J Geophys Res 100:22435–22446

Hayes DE, Nissen SS (2005) The South China sea margins: Implications for rifting contrasts. Earth Planet Sci Lett 237:601–616

Ho CS (1986) A synthesis of the geological evolution of Taiwan. Tectonophysics 25:1–16

Holloway NH (1982) North Palawan Block, Philippines -its relation to the Asian mainland and role in evolution of South China Sea. AAPG Bull 66:1355–1383

Hsu S-K, Liu C-S, Shyu C-T, Liu S-Y, Sibuet J-C, Lallemand S, Wang C-S, Reed D (1998) New gravity and magnetic anomaly maps in the Taiwan-Luzon region and their preliminary interpretation. Terr Atmos Ocean Sci 9:509–532

Hsu S-K, Sibuet J-C (1995) Is Taiwan the result of arc-continent or arc-arc collision? Earth Planet Sci Lett 136:315–324

Huang C-Y, Xia K-Y, Yuan PB, Chen P-G (2001) Structural evolution from Paleogene extension to Latest Miocene-Recent arc-continent collision offshore Taiwan: comparison with on land geology. J Asian Earth Sci 19:619–639

Jahn BM, Chen PY, Yen TP (1976) Rb–Sr ages of granitic rocks in southeastern China and their tectonic significance. Bull Geol Soc Am 86:763–776

Jones TD, Nur A (1984) The nature of seismic reflections from deep crustal fault zones. J Geophys Res 89:3153–3171

Kao H, Huang G-C, Liu C-S (2000) Transition from oblique subduction to collision in the northern Luzon arc-Taiwan region: constraints from bathymetry and seismic observations. J Geophys Res 105:3059–3079

Kido Y, Suyehiro K, Kinoshita H (2001) Rifting to spreading process along the northern margin of the South China Sea. Mar Geophys Res 22:1–15

Kizaki K (1986) Geology and tectonics of the Ryukyu islands. Tectonophysics 125:193–207

Lacombe O, Mouthereau F, Angelier J, Deffontaines B (2001) Structural, geodetic and seismological evidence for tectonic escape in SW Taiwan. Tectonophysics 333:323–345

Lapierre H, Jahn BM, Charvet J, Yu YW (1997) Mesozoic felsic arc magmatism and continental olivine tholeiites in Zhejiang Province and their relationship with the tectonic activity in southeastern China. Tectonophysics 274:321–338

Lee T-Y, Lawver LA (1995) Cenozoic plate reconstruction of Southeast Asia. Tectonophysics 251:85–138

Lee T-Y, Tang C-H, Ting J-S, Hsu Y-Y (1993) Sequence stratigraphy of the Tainan Basin, offshore southwestern Taiwan. Pet Geol Taiwan 28:119–158

Leloup PH, Arnaud N, Lacassin R, Kienast JR, Harrison TM, Trinh PT, Replumaz A, Tapponnier P (2001) New constrains on the structure, thermochronology and timing of the Ailao Shan—Red River shear zone. J Geophys Res 106:6683–6732

Lesne O, Calais E, Deverchère J, Hassani R, Chery J (2000) Dynamics of intracontinental extension in the North Baikal rift from two-dimensional numerical deformation modelling. J Geophys Res 105:21727–21744

Li C-F (2004) Comparative geological study between the western Pacific marginal seas and the paleo-Tethyan marginal seas. In: Li J, Gao S (eds) Basin Evolution and Resources of the Chinese Marginal Seas, (Vol 3, Serial studies of the formation and evolution of the Chinese marginal seas). Ocean Press, Beijing, pp 46–53, color plate III, IV (in Chinese)

Li C-F, Zhou Z, Li J, Chen H, Geng J, Li H (2007) Precollisional tectonics and terrain amalgamation offshore southern Taiwan: Characterizations from reflection seismic and potential field data. Sci China Ser D Earth Sci (In press)

Li Q, Jian Z, Li B (2004) Oligocene-Miocene planktonic foraminifer biostratigraphy, Site 1148, northern South China Sea. In: Prell WL, Wang P, Blum P, Rea DK, Clemens SC (eds) Proc ODP, Sci Results 184: 1–26 (Online)

Lin AT, Watts AB (2002) Origin of the West Taiwan basin by orogenic loading and flexure of a rifted continental margin. J Geophys Res 107. DOI 10.1029/2001JB000669

Lin AT, Watts AB, Hesselbow SP (2003) Cenozoic stratigraphy and subsidence history of the South China Sea margin in the Taiwan region. Basin Res 15:453–478

Ludwig WJ, Nafe JE, Drake CL (1970) Seismic refraction. In: Maxwell AE (ed) The Sea, Vol 4. Wiley-Interscience, New York, pp 53–84

Miki M (1995) Two-phase opening model for the Okinawa Trough inferred from paleomagnetic study of the Ryukyu Arc. J Geophys Res 100:8169–8184

Nakamura Y, McIntosh K, Chen AT (1998) Preliminary results of a large offset seismic survey west of Hengchun Peninsula, southern Taiwan. Terr Atmos Ocean Sci 9:395–408

Nissen SS, Hayes DE, Buhl P, Diebold J, Yao B, Zeng W, Chen Y (1995a) Deep penetration seismic soundings across the northern margin of the South China Sea. J Geophys Res 100:22407–22433

Nissen SS, Hayes DE, Yao B, Zeng W, Chen Y, Nu X (1995b) Gravity, heat flow, and seismic constraints on the processes of crustal extension: northern margin of the South China Sea. J Geophys Res 100:22447–22483

Pautot G, Rangin C, Briais A, Tapponnier P, Beuzart P, Lericolais G, Mathieu X, Wu J, Han S, Li H, Lu Y, Zhao J (1986) Spreading direction in the central South China Sea. Nature 321:150–154

Qiu X, Ye S, Wu S, Shi X, Zhou D, Xia K, Flueh ER (2001) Crustal structure across the Xisha Trough, northwestern South China Sea. Tectonophysics 341:179–193

Reston TJ, Krawczyk CM, Klaeschen D (1996) The S reflector west of Galicia (Spain): Evidence from prestack depth migration for detachment faulting during continental breakup. J Geophys Res 101:8075–8091

Ru K, Pigott JD (1986) Episodic rifting and subsidence in the South China Sea. AAPG Bull 70:1136–1155

Sandwell DT, Smith WHF (1997) Marine gravity anomaly from Geosat and ERS 1 satellite altimetry. J Geophys Res 102:10039–10054

Seno T, Stein S, Gripp AE (1993) A model for the motion of the Philippine Sea plate consistent with NUVEL-1 and geological data. J Geophys Res 98:17941–17948

Shinjo R (1999) Geochemistry of high Mg andesites and the tectonic evolution of the Okinawa Trough - Ryukyu arc system. Chem Geol 157:69–88

Sibuet J-C, Hsu S-K (1997) Geodynamics of the Taiwan arc-arc collision. Tectonophysics 274:221–251

Sibuet J-C, Hsu S-K, Debayle E (2004) Geodynamic context of the Taiwan orogen. In: Clift P, Wang P, Kuhnt W, Hayes D (eds) Ocean-Continent Interactions within East Asian Marginal Seas, vol 149. Am Geophys Union Monogr, pp 127–158

Sibuet J-C, Hsu S-K, Le Pichon X, Le Formal J-P, Reed D, Moore G, Liu C-S (2002) East Asia plate tectonics since 15Ma: constraints from the Taiwan region. Tectonophysics 344:103–134

Su D, White N, McKenzie D (1989) Extension and subsidence of the Pearl River Mouth basin, northern South China Sea. Basin Res 2:205–222

Suppe J (1984) Kinematics of arc-continent collision, flipping of subduction, and back-arc spreading near Taiwan. Mem Geol Soc China 6:21–34

Talwani M, Worzel JL, Landisman M (1959) Rapid gravity computations for two-dimensional bodies with application to the Mendocino submarine fracture zone. J Geophys Res 64:49–59

Tang J-C, Chemenda AI (2000) Numerical modeling of arc-continent collision: application to Taiwan. Tectonophysics 325:23–42

Tapponnier P, Peltzer G, Le Dain AY, Armijo R, Cobbold P (1982) Propagating extrusion tectonics in Asia: new insights from simple experiments with plasticine. Geology 7:611–616

Taylor B, Hayes DE (1980) The tectonic evolution of the South China Sea. In: Hayes DE (ed) The Tectonic and Geologic Evolution of South Eastern Asian Seas and Islands, I. Am Geophys Union, Geophys Monogr, Washington, DC, 23, pp 89–104

Taylor B, Hayes DE (1983) Origin and history of the South China Sea basin. In: Hayes DE (Ed) The Tectonic and Geologic Evolution of South Eastern Asian Seas and Islands, II. Am Geophys Union, Geophys Monogr, Washington, DC, 27, pp 23–56

Teng LS (1990) Geotectonic evolution of the late-Cenozoic arc-continent collision in Taiwan. Tectonophysics 183:57–76

Teng LS (1996) Extensional collapse of the northern Taiwan mountain belt. Geology 24:949–952

Tommasi A, Vauchez A (2001) Continental rifting parallel to ancient collisional belts: an effect of the mechanical anisotropy of the lithospheric mantle. Earth Planet Sci Lett 185:199–210

Tzeng J (1994) Tertiary Seismic Stratigraphic Analysis of the Tainan Basin. M.S. Thesis, National Taiwan University (in Chinese)

Wang K-L, Chung S-L, Chen C-H, Shinjo R, Yang TF, Chen C-H (1999) Post-collisional magmatism around northern Taiwan and its relation with opening of the Okinawa Trough. Tectonophysics 308:363–376

Wang P, Prell WL, Blum P, Arnold EM, Buehring CJ, Chen M-P, Clemens SC, Clift PD, Colin CJG, Farrell JW, Higginson MJ, Jian Z, Kuhnt W, Laj CE, Lauer-Leredde C, Leventhal JS, Li A, Li Q, Lin J, McIntyre K, Miranda CR, Nathan SA, Shyu J-P, Solheid PA, Su X, Tamburini F, Trentesaux A, Wang L (2000a) Proceedings of Ocean Drilling Program, Initial Report, 184. College Station, TX: Ocean Drilling Program

Wang P, Xia K, Huang C (2000b) Distribution and geological & geophysical characteristics of Mesozoic marine strata in northeastern part of South China Sea. Tropic Oceanology 19:28–35 (in Chinese)

Warner M, Morgan J, Barton P, Morgan P, Price C, Jones K (1996) Seismic reflections from the mantle represent relict subduction zones within the continental lithosphere. Geology 24:39–42

Wessel P, Smith WHF (1995) New version of the Generic Mapping Tools (GMT) version 3.0 released, Trans AGU, EOS 76: 329

Wilson JT (1966) Did the Atlantic close and then re-open? Nature 211:676–681

Wu FT, Rau R-J, Salzberg D (1997) Taiwan orogeny: thin-skinned or lithospheric collision? Tectonophysics 274:191–220

Xia K et al (1997) Geophysical field and crustal structures of the South China Sea. In: Gong Z, Li S et al (Eds) Continental margin basin analysis and hydrocarbon accumulation of the Northern South China Sea. Science Press, Beijing, pp 1–16 (in Chinese)

Xia K, Huang C (2000) The discovery of Meso-Tethys sedimentary basins in the South China Sea and their oil and gas perspective. Earth Sci Frontiers 7:227–238 (in Chinese)

Xia K-Y, Huang C-L, Jiang S-R, Zhang Y-X, Su D-Q, Xia S-G, Chen Z-R (1994) Comparison of tectonics and geophysics of the major structural belts between the northern and southern continental margins of the South China Sea. Tectonophysics 235:99–116

Yan P, Zhou D, Liu Z (2001) A crustal structure profile across the northern continental margin of the South China Sea. Tectonophysics 338:1–21

Yang TF, Lee T, Chen C-H, Cheng S-N, Knittel U, Punongbayan RS, Rasdas AR (1996) A double island arc between Taiwan and Luzon: consequence of ridge subduction. Tectonophysics 258:85–101

Yao B (1996) Tectonic characteristics and evolution of the Nansha Trough. Geol Res South China Sea Memoir 8:1–13 (in Chinese)

Yao B, Zeng W, Hayes DE, Spangler S et al (1994) The Geological Memoir of South China Sea Surveyed Jointly by China and USA. China University of Geosciences Press, p 204 (in Chinese)

Yu S-B, Chen H-Y, Kuo L-C (1997) Velocity field of GPS stations in the Taiwan area. Tectonophysics 274:41–59

Zhou XM, Li WX (2000) Origin of late Mesozoic igneous rocks in southeastern China: implications for lithosphere subduction and underplating of mafic magmas. Tectonophysics 326:269–287

Zhou Z, Lao Q, Chen H, Ding S, Liao Z (1996) Early Mesozoic orogeny in Fujian, Southeast China. In: Hall R, Blundell D (eds) Tectonics Evolution of Southeast Asia, vol 106. Geol Soc Spec Publ, pp 549–556